2440–2451 *Nucleic Acids Research, 2022, Vol. 50, No. 5* *Published online 2 March 2022*
https://doi.org/10.1093/nar/gkac139

Small molecule targeting CELF1 RNA-binding activity to control HSC activation and liver fibrosis

Yang Tan[1,†], Xueqing Sun[1,†], Yizhu Xu[1,†], Bingjie Tang[1], Shuaiqi Xu[1], Dong Lu[2], Yan Ye[2], Xiaomin Luo[2,3], Xu Diao[4], Fulong Li[5], Tianyi Wang[1], Jiayu Chen[6], Qiang Xu[1,*] and Xingxin Wu[1,*]

[1]State Key Laboratory of Pharmaceutical Biotechnology, School of Life Sciences, Nanjing University, Nanjing, Jiangsu 210023, China, [2]Drug Discovery and Design Center, State Key Laboratory of Drug Research, Shanghai Institute of Materia Medica, Chinese Academy of Sciences, Shanghai 201203, China, [3]University of Chinese Academy of Sciences, 19 Yuquan Road, Beijing 100049, China, [4]Department of Pharmacology, Jiangsu Simovay Pharmaceutical Co., Ltd., Nanjing, Jiangsu 210042, China, [5]Department of Pharmaceutical Chemistry, Jiangsu Simovay Pharmaceutical Co., Ltd., Nanjing, Jiangsu 210042, China and [6]State Key Laboratory of Pharmaceutical Biotechnology, School of Life Sciences, Chemistry and Biomedicine Innovation Center (ChemBIC), Nanjing University, Nanjing 210023, China

Received September 08, 2021; Revised January 21, 2022; Editorial Decision February 11, 2022; Accepted February 14, 2022

ABSTRACT

CUGBP Elav-like family member 1 (CELF1), an RNA-binding protein (RBP), plays important roles in the pathogenesis of diseases such as myotonic dystrophy, liver fibrosis and cancers. However, targeting CELF1 is still a challenge, as RBPs are considered largely undruggable. Here, we discovered that compound 27 disrupted CELF1-RNA binding via structure-based virtual screening and biochemical assays. Compound 27 binds directly to CELF1 and competes with RNA for binding to CELF1. Compound 27 promotes IFN-γ secretion and suppresses TGF-β1-induced hepatic stellate cell (HSC) activation by inhibiting CELF1-mediated IFN-γ mRNA decay. *In vivo*, compound 27 attenuates CCl_4-induced murine liver fibrosis. Furthermore, the structure-activity relationship analysis was performed and compound 841, a derivative of compound 27, was identified as a selective CELF1 inhibitor. In conclusion, targeting CELF1 RNA-binding activity with small molecules was achieved, which provides a novel strategy for treating liver fibrosis and other CELF1-mediated diseases.

INTRODUCTION

CUGBP Elav-like family member 1 (CELF1), an RNA binding protein (RBP), plays important roles in various diseases, including myotonic dystrophy (1), dilated cardiomyopathy (2), tumour metastasis (3) and liver fibrosis (4). CELF1 binds to GU-rich elements in mRNA and regulates mRNA splicing, translation and decay (5–10). In myotonic dystrophy type 1 (DM1), a CTG repeat expansion mutation in the 3′UTR of DM protein kinase (DMPK) leads to nuclear accumulation of CELF1, which causes mRNA dysregulation (11). In dilated cardiomyopathy, elevated CELF1 promotes Cx43 mRNA degradation by binding GU-rich elements in the 3′UTR of Cx43, which causes cardiac phenotypes in the infarcted heart (2). CELF1 functions as a central node to regulate translational activation of EMT genes and drive tumour progression (3). Previously, we found that CELF1 promoted hepatic stellate cell (HSC) activation and liver fibrosis by inducing antifibrotic IFN-γ mRNA decay (4,12–14). CELF1 expression is selectively upregulated in activated HSCs. Knockdown of CELF1 expression attenuates murine liver fibrosis (4). These findings suggest that CELF1 is an attractive target for treating various diseases, including liver fibrosis. However, no inhibitor targeting CELF1 has been reported.

RBPs are rapidly emerging as therapeutic targets (15–22). However, targeting RBPs with small molecules is still a challenge because most RBPs are considered undruggable due to a lack of well-defined binding pockets (18). One strategy to block the function of RBPs is to target their RNA binding activity by disrupting the interaction between the RBP and its target RNA (16). The binding characteristics between CELF1 and GU-rich elements have been discovered (11,23–25). CELF1 harbours three RNA recognition motifs (RRMs). The first two RRMs (RRM1/2) of CELF1 are capable of binding independently to a single

*To whom correspondence should be addressed. Tel: +86 25 8968 5074; Email: xingxin.wu@nju.edu.cn
Correspondence may also be addressed to Qiang Xu. Tel: +86 25 8968 1312; Email: molpharm@163.com
†The authors wish it to be known that, in their opinion, the first three authors should be regarded as joint First Authors.

UGU site. A structural study showed that both RRM1 and RRM2 bind UGU(U/G) elements in a highly similar way (26). Phe19/Phe111, Gln22/Met114, Cys61/Cys150, Phe63/Phe152, Gln93/Val182 and Asp98/Asp187 residues mediate intermolecular contacts in the crystal structures of RRM1/2-RNA complexes. Thus, we think targeting the binding surface between RRM1/2 and the UGUU element may block CELF1 RNA-binding activity.

Here, by combining *in silico* screening and biochemical assays, we discovered that small molecule compound **27** was a disruptor of CELF1-RNA binding. Compound **27** binds to CELF1 to compete with RNA. Compound **27** inhibits CELF1-mediated IFN-γ mRNA decay and controls HSC activation. *In vivo*, compound **27** attenuates CCl_4-induced murine liver fibrosis. Furthermore, the structure-activity relationship analysis was performed and compound **841**, a derivative of compound **27**, was identified as a selective CELF1 inhibitor. In conclusion, we discovered CELF1 RNA-binding inhibitors that maintain HSC homeostasis for the treatment of liver fibrosis.

MATERIALS AND METHODS

Virtual screening

The crystal structure of CELF1 (PDB: 3NMR) was prepared in the protein preparation Wizard Workflow of Schrodinger software package (Schrodinger LLC, New York, NY, 2010). All crystal water molecules were deleted from the structure. The structure was then minimized with the OPLS_2005 force field. Then, a three-dimensional receptor grid was generated at guanosine site using the Receptor Grid Generation module from the Maestro software (Schrodinger LLC, New York, NY, 2010). The other parameter values were assigned to default.

The commercial Specs database (https://www.specs.net) was selected for virtual screening. Compounds containing PAINS or violating 'Lipinski's Rule of Five' were removed from the compound library. LigPrep (version 2.4, Schrödinger, LLC, New York, NY, 2010) was used to generate stereoisomers and tautomer, and the stereoisomers were generated at most 32 per ligand. The protonation states of ligands at pH 7.0 ± 2.0 were generated with Epik. The prepared receptor and ligand files were imported into the Ligand Docking module using the Glide module of Maestro software (Glide, version 6; Schrödinger LLC, New York, NY, 2010) with the standard precision mode (SP) (27). The top-ranked 10 000 poses were grouped into 100 clusters. The similarity between two compounds was calculated using the Tanimoto coefficient of ECFP4 fingerprint (28). After visual inspection of the binding poses of these compounds, 90 molecules with structural diversity and shape rationality were selected and purchased for further biological assay evaluation.

Mice

Eight-week-old male ICR mice were supplied by the Experimental Animal Center of Yangzhou University (Yangzhou, China). All of the male ICR mice received humane care according to the criteria outlined in the 'Guide for the Care and Use of Laboratory Animals' prepared by the National Academy of Sciences and published by the National Institutes of Health. All animal experimental procedures were approved by the Animal Care Committee of Nanjing University (Nanjing, China).

Cell culture

The human hepatic stellate cell line LX-2 was purchased from Xiang Ya Central Experiment Laboratory, Central South University, China. LX-2 cells were cultured in Dulbecco's modified Eagle's medium with 2% fetal bovine serum, Primary HSCs were isolated from the mouse liver according to a reported protocol and cultured in n Dulbecco's modified Eagle's medium with 10% fetal bovine serum. All cells cultured under a humidified 5% (v/v) CO_2 atmosphere at 37°C.

CELF1 RRM1/2 protein expression

CELF1 RRM1/2 (1–187 aa) containing 8*His tag at N-terminal was cloned into pET28b (+) vector with NcoI and EagI restriction sites. All proteins were overexpressed in Escherichia coli BL21 (DE3) cells grown in Luria Broth media. All media was treated with 50 μg/ml kanamycin. Protein expression was induced for 16 h at 30°C. Harvested cells were lysed by sonication in 50 mM Tris, 50 mM NaCl, pH 7.5 buffer. A protease inhibitor cocktail was added immediately before sonication.

Fluorescence polarization (FP) assay

RNA probes labeled with 3′Cy3 with the following sequences were purchased from GenScript: GU Probe, 5′-UUGUUGUU-3′; Random Probe, 5′-GUUUAUGU-3′, Initial optimization experiments were performed in 96-well black plates (Corning) using the TECAN spark plate reader. For assay optimization and determination of the equilibrium dissociation constant, CELF1 RRM1/2 and 10 nM fluorescein labeled RNA probes were added to the assay buffer (25 mM Tris pH 7.5, 25 mM NaCl, and 1% (v/v) Tween-20) with a final volume of 150 μl and incubated at RT for 30 min. For the compound screening assay, compounds at 100 μM were added to the wells prior to the protein−RNA complex. For the compound competition assay, compounds with Ten doses (0.39−200 μM) were added to the wells prior to the protein−RNA complex. Polarization measurements were taken after incubation at RT for 30 min.

Electrophoresis mobility shift assay (EMSA)

Compound 27 was pre-incubated with 50 nM CELF1 RRM1/2/3 for 10 min at room temperature and followed with adding 50 nM Rox labeled oligonucleotide RNA probe in assay buffer (25 mM Tris pH 7.5, 25 mM NaCl, and 1% (v/v) Tween-20). Samples were run in non-denatured glue and gel shift was detected with IE800 (Cytiva, USA)

Isothermal titration calorimetry

ITC measurements were collected using a Microcal VP-ITC calorimeter. All experiments were performed at 25°C. An

amount 40 μM solution of the protein injected from the syringe. The titration consisted of 20 injections of 10 μl each at 2-min intervals. Data was analysed using the Microcal ORIGIN software.

Flow cytometry analysis

Stable transfection of dual fluorescence reporter (OBiO Technology, China) cells are plated into 12-well plates with 1×10^5 cells per well. 20 μM compounds was added and treated for 24 h. Cells were corrected for detecting EGFP/mCherry fluorescence intensity. Flow cytometry analysis was performed on Attune NxT Cytometer.

Enzyme-linked immunosorbent assay

LX-2 cells were treated with 20 μM compound **27** for 24 h and the cell supernatant was collected for ELISA assay. ELISA kit for human IFN-γ was bought from BD company (555142). 96-well microplates were bought from Thermo Nunc (436110). ELISA assays were carried out according to the instructions.

Western blot analysis

Proteins were extracted from LX-2 cells in the lysis buffer. Antibodies used in western blot were: Goat Anti-Type I Collagen-AF488 (Southern Biotech, 1310-30, 1:1000 dilution), CELF1 (Santa Cruz Biotechnology, SC-20003, 1:1000 dilution), α-SMA (Santa Cruz Biotechnology, SC-32251, 1:1000 dilution), anti-β-tubulin (Abmart, M20005M, 1:1000 dilution), GAPDH (Abmart, AM1021B, 1:1000 dilution). The relative expressions were quantified according to the reference bands of β-tubulin or GAPDH.

Immunofluorescence cytochemistry

Mouse primary HSCs adhered to glass were fixed with 4% paraformaldehyde (40 min, room temperature). Cells were further stained with the following antibodies: α-SMA (Santa Cruz Biotechnology, SC-32251, 1:50) detected with secondary antibodies: goat anti-mouse IgG2a conjugated to Alexa Fluor 594 (Invitrogen, A-21135, 1:1000). The coverslips were counterstained with DAPI and imaged with a confocal laser scanning microscope (Olympus, Lake Success, NY). Examination was blindly carried out.

Reverse transcriptase-PCR and quantitative PCR

Total RNA was extracted from LX-2 cells using Tripure reagent (Roche Diagnostics, Indianapolis, IN) as described by the manufacturer. Single-stranded cDNA was synthesized from 2 μg of total RNA by reverse transcription using 0.5 μg of oligo (dT) 18 primer. PCR was performed at 94°C for 30 s, 58°C for 1 min and 72°C for 1 min. The level of GAPDH RNA expression was used to normalize the data. The primers used for quantitative PCR are described in Supplementary Table S1.

RNA interference

Transfections were performed with Lipofectamine RNAiMAX transfection Reagent (13778150) (Invitrogen, Carlsbad, CA) according to the manufacturer's recommendations. CELF1-specific siRNA (1299003) and non-silencing siRNA (12935200) (Invitrogen, Carlsbad, CA) were transfected on cells with a siRNA concentration of 100 nM.

Tissue sirius red staining

Formalin fixed and paraffin embedded liver fibrosis tissue arrays were cut 5 μm. Sirius Red staining was performed by Servicebio (Wuhan, China). The liver fibrosis stage was assessed by Ishak scale.

Hydroxyproline content assay

The hydroxyproline content in the liver was determined by the spectrophotometric method according to the hydroxyproline assay kit's instruction manual. The data are expressed as Hyp (μg) per wet liver weight (g).

In well protein RNA-binding assay

293T cells were transfected with indicated CELF member plasmids containing Flag tag and the cell lysates were collected. In well protein RNA-binding assay was performed on 96-well microplates (Thermo Nunc, 436110) pre-coated with 100 μg/ml Strepavidin (NEB, 7021S). Compound 27 mixed with 10 nM Biotin-GU RNA and some amount cell lysate were added to the wells and incubate for 30 min at room temperature. Wash three times with PBST and then incubate with HRP conjugated anti-Flag antibody for another 30 min at room temperature. Wash five times with PBST and incubate with TMB ELISA substrates. Stop the reaction with stop solution and detect with microplate reader.

Statistical analysis

Statistically evaluated by Student's t test with two-tailed test when only two value sets were compared, and one-way analysis of variance followed by Dunnett's test when the data involved three or more groups. $P < 0.05$ was considered significant.

RESULTS

The RRM1/2 of CELF1 is targeted by a small molecule compound 27 that disrupts CELF1-RNA binding

The crystal structure of CELF1 with RNA (PDB ID: 3NMR) was evaluated to screen small molecule inhibitors of CELF1 RNA-binding activity. The small molecule binding site of CELF1 RRM2 was settled for competing RNA binding (Figure 1A). The overall workflow of virtual screening is shown in Figure 1B. We chose a commercially available Specs database as the ligand library. Lipinski's rule of five and pan-assay interference structure (PAINS) were used to filter the data, and the remaining 100,000 compounds

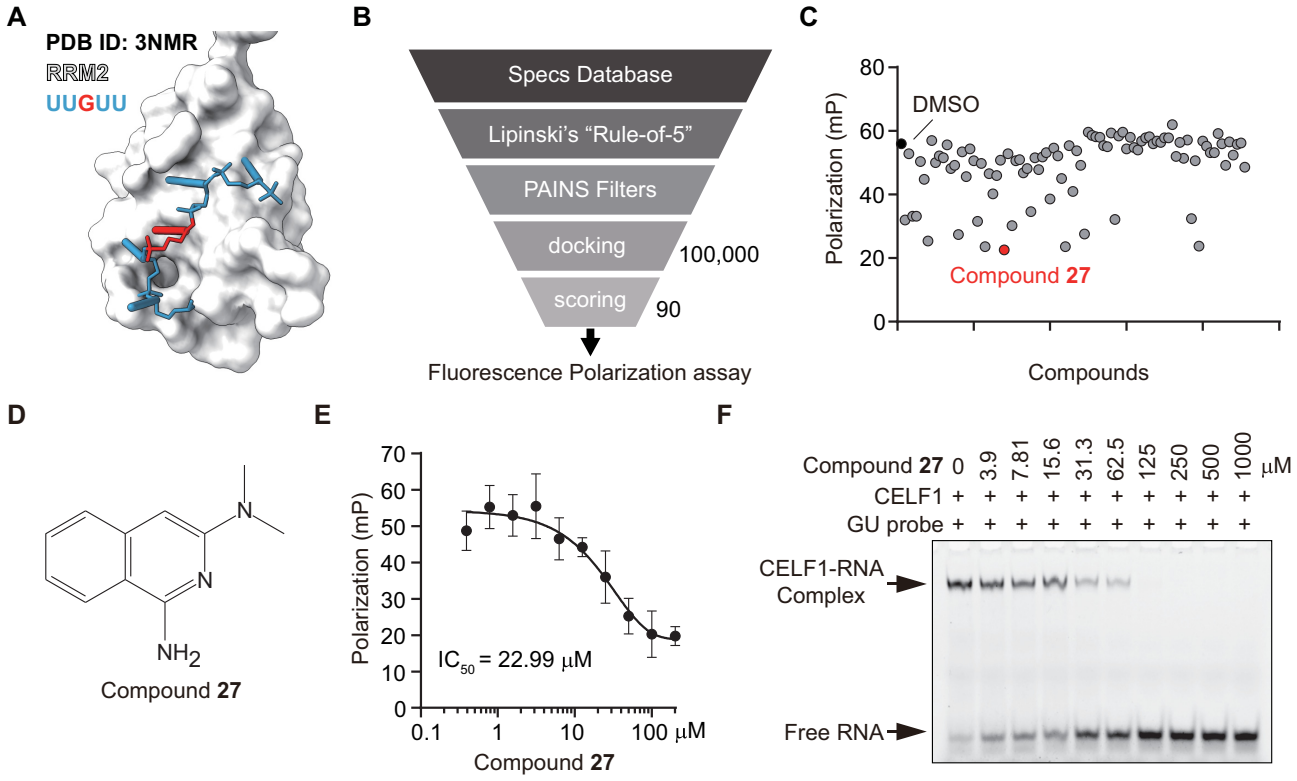

Figure 1. Identification of compound 27 as a small molecule inhibitor to disrupt the CELF1–RNA interaction. (**A**) Surface representations of the crystal structures of RRM1/2 of CELF1 (PDB ID: 3NMR) bound to RNA. (**B**) The workflow of virtual screening. (**C**) FP values for the 90 screened compounds. (**D**) Chemical structure of compound **27**. (**E**) FP values of compound **27** for RRM1/2-RNA binding inhibition. (**F**) RRM1/2 was pre-treated with compound **27** at indicated concentrations and then incubated with a 50 nM fluorescein labelled RNA probe. The position of migration of the probe bound to RRM1/2 is indicated with an arrow. Error bars in **E** depict mean ± SD.

were prepared and docked into the binding site of the prepared CELF1 RRM2. The top-ranked 10 000 molecules were selected and clustered into 90 groups. According to the scoring results, we selected the top 90 molecules for further biochemical analysis. To evaluate the disrupting activity of 90 molecules, we designed a FP assay. We generated an 8-nt GU probe containing the known CELF1 recognition motif (UUGUU) and a single Cyanine 3 fluorescein label ligated to the 3′-end (Supplementary Figure S1A). Recombinant RRM1/2 (aa 1–187) of CELF1 was titrated with GU probe and examined by FP, which demonstrated that RRM1/2 associates with the GU probe (Supplementary Figure S1B–D). Titration with increasing amounts of unlabeled cold probe demonstrated the reversibility and specificity of the association (Supplementary Figure S1E).

Next, a FP screening was performed to determine the competitive activity of the selected compounds with a GU-rich probe. The FP values of 90 compounds against RRM1/2 are shown in Figure 1C. Compound **27** showed the highest competitive activity, with an IC50 value of 22.99 μM (Figure 1D and E). Further, EMSA was chosen as an orthogonal assay to evaluate compound **27** in dose response. A 19-nt RNA probe was generated and its binding with CELF1 RRM1/2/3 was detected by EMSA (Supplementary Figure S2). Compound **27** disrupted the RRM1/2/3-RNA interaction in a dose-dependent manner (Figure 1F). To evaluate the specificity of compound **27**, we selected HuR, an AU binding protein for further test. Our data indicate that the compound **27** did not disrupt HuR-RNA binding activity in FP assay (Supplementary Figure S3A–C). Consistently, compound **27** did not affect the mRNA stability of *MMP9* and *VEGFA*, two well-known HuR targets (29,30) (Supplementary Figure S3D). Therefore, compound **27** was chosen as a hit compound for further study.

Compound 27 binds to CELF1 mainly at K117 and competes with GU-rich RNA

To investigate whether compound **27** directly bound to CELF1, a putative binding mode of compound **27** with RRM2 of CELF1 was generated by Schrödinger software. The amino acids Lys117, Arg148 and Cys177 were predicted as putative residues of CELF1 RRM2 for compound **27** binding (Figure 2A). The binding poses of compound **27** were similar to the poses of RNA binding to RRM2 (Figure 2B). To directly test our docking model, we mutated the putative interacting residues (K117A, R148A and C177A) and determined their ability to bind to compound **27** by using isothermal titration calorimetry (ITC). The

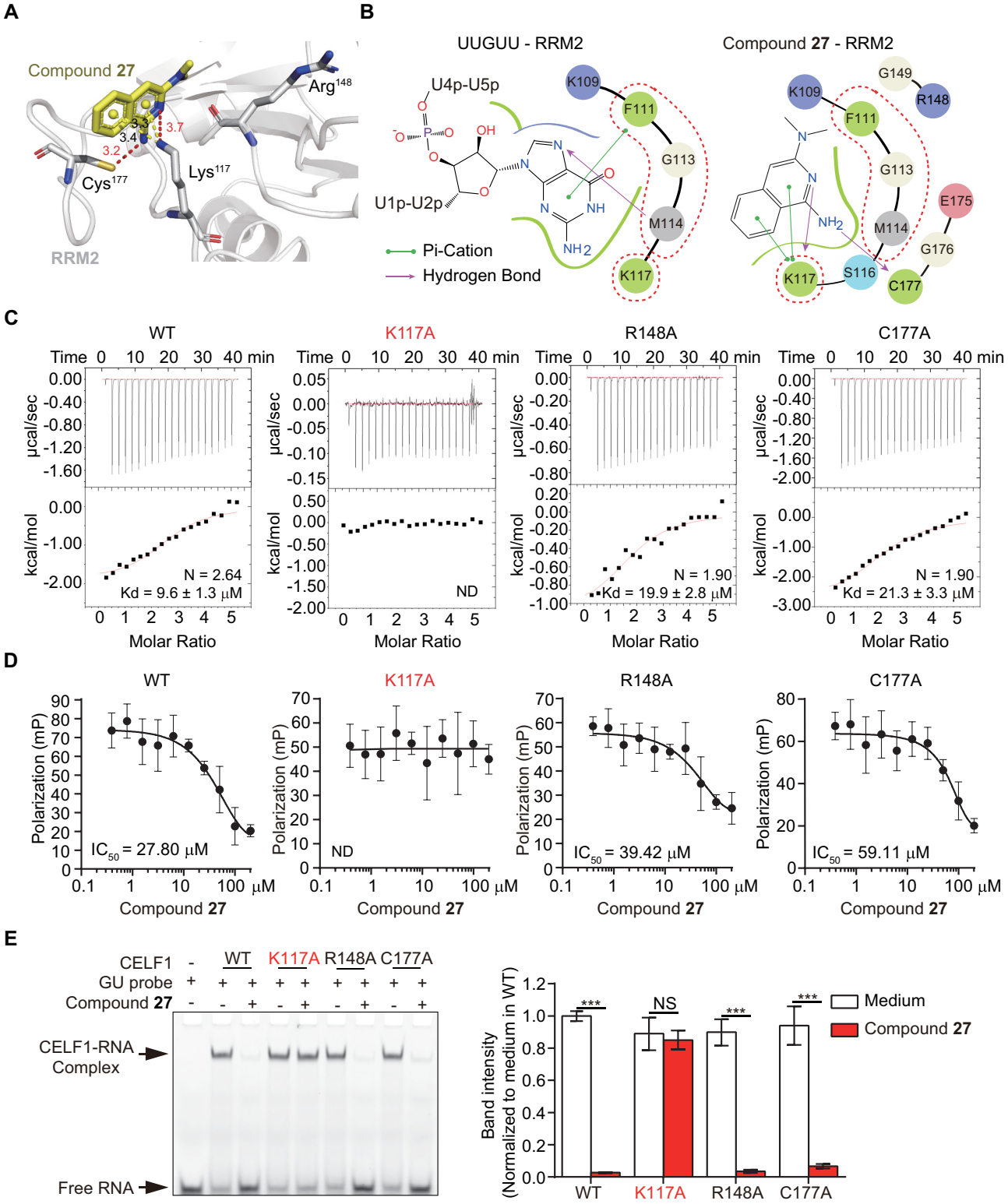

Figure 2. Compound 27 directly interacts with CELF1 mainly at K117 and competes with GU-rich RNA. (**A**) Docking mode of compound **27** with the relevant interaction residues (Lys117, Cys177) and distances (Å) between them. (**B**) 2D representation of residues involved in UUGUU RNA and compound **27** binding with RRM2. (**C**) Comparison of ITC profiles of RRM1/2 (WT, K117A, R148A and C177A) titrated with compound **27**. (**D**) FP values for compound **27** with RRM1/2 (K117A, R148A and C177A). (**E**) Gel shift assay of compound **27** with RRM1/2/3 (WT, K117A, R148A and C177A). The data are representative of three independent experiments (mean ± SD). ***$P < 0.001$ by Student's *t*-test, NS, not significant.

CELF1 S147A mutation, which was not predicted to disrupt CELF1–RNA interaction, was taken as a negative control. The CELF1 K117A mutants had significantly decreased binding to compound **27** (K117A: K_d value not detected; R148A: K_d 19.9 ± 2.8 μM; C177A: K_d 21.3 ± 3.3 μM, compared with 9.6 ± 1.3 μM for wild-type (WT) and 9.2 ± 1.6 μM for S147A) (Figure 2C and Supplementary Figure S4), suggesting the residue K117 is critical for the binding. Consistent with the ITC results, compound **27** was not able to inhibit the binding between K117A mutant CELF1 and RNA, as shown by FP and EMSA (Figure 2D and E). Importantly, we experimentally validate that K117A single mutation could decrease interaction between RRM1/2 and GU probe in FP assay (Supplementary Figure S5). These data suggest that the K117 residue of CELF1 was critical for the inhibition of CELF1 RNA-binding by compound **27**.

We further examine the binding affinity of compound **27** to various RNAs to check the possibility that compound **27** disrupts CELF1–RNA interaction by binding to RNA. Using ITC, we found compound **27** did not bind to UUGUUGUU or $(CUG)_8$ (Supplementary Figure S6). Overall, these data suggest that compound **27** is selectively binding to CELF1 to competing GU RNA.

Compound 27 inhibits HSC activation via preventing CELF1-mediated IFN-γ mRNA degradation

One function of CELF1 is to mediate mRNA degradation. IFN-γ mRNA is a CELF1 substrate and IFN-γ plays an antifibrogenic role in liver fibrosis (14,31,32). CELF1 mediates IFN-γ mRNA degradation by binding to GU-rich elements in the 3′UTR of IFN-γ mRNA (4). To further monitor if compound 27 attenuates CELF1 mediated mRNA decay in living cell, we generated an EGFP/mCherry-based dual fluorescence reporter. In this reporter, the IFN-γ mRNA 3′UTR was cloned downstream of EGFP, and mCherry was used as an internal reference (Figure 3A). Knockdown of CELF1 by small interfering RNA significantly increased the EGFP/mCherry ratio, which suggests that the reporter is a good tool for examining CELF1 activity (Figure 3B). Furthermore, compound **27** significantly increased the EGFP intensity but had no effect on the mCherry intensity, suggesting that compound **27** may effectively inhibit IFN-γ mRNA expression (Figure 3C). Further, we examined RNA stability of CELF1 targets. Besides IFN-γ, another well-known CELF1 targets c-JUN was included here to confirm that compound **27** can block the CELF1 function (8). In line with expectation, compound **27** protected IFN-γ and c-JUN mRNA from degradation in LX-2 cells (Figure 3D). In addition, the ELISA results showed that compound **27** increased IFN-γ protein levels in LX-2 cell supernatants accompanying with increased IFN-γ mRNA (Figure 3E and F).

Compound 27 attenuates CCl_4-induced murine liver fibrosis

HSC activation is a key step in liver fibrogenesis and CELF1 is a key regulator that contributes to HSC activation accompanied by increased α-SMA and collagen I(α)1 (4,12). To determine whether compound **27** attenuated HSC activation, we examined the effects of compound **27** on the activation of LX-2 cells and primary murine HSCs by evaluating α-SMA and collagen I(α)1 expression. In LX-2 cells, compound **27** significantly inhibited α-SMA and collagen I(α)1 protein expression, while compound **21**, a negative control, did not induce inhibition (Figure 4A). In primary murine HSCs, compound **27** also reduced α-SMA protein expression (Figure 4B). Consistently, compound **27** downregulated *ACTA2* and *COL1A1* mRNA expression (Figure 4C). But compound **27** failed to reduce collagen *I*(α)1 expression in CELF1-knockdown LX-2 cells (Figure 4D). These data suggested that compound **27** inhibited HSC activation in a CELF1-dependent manner.

Next, we generated a CCl_4-induced murine liver fibrosis model to test whether compound **27** attenuates liver fibrosis *in vivo*. To determine the dosage and method of administration, pharmacokinetics and pharmacodynamics researches of compound **27** were carried out (Supplementary Figure S7). Two doses (1 mg/kg and 3 mg/kg) of compound **27** were administered daily by intraperitoneal injection, and colchicine was used as a positive control. Compound **27** induced a marked reduction in the fibrotic surface (Figure 4E). In line with the histological analysis, the mRNA expression of profibrotic genes (including *α-SMA* and *Col1a1*) further demonstrated that compound **27** was effective against liver fibrosis (Figure 4F). Consistently, the administration of compound **27** significantly reduced serum ALT, AST and tissue hydroxyproline levels (Figure 4G). Overall, these results suggested that compound **27** exerted a protective effect against CCl_4-induced liver fibrosis in mice.

Compound 841, a derivative of compound 27, selectively inhibits CELF1 RNA-binding activity

To test structure-activity relationships, we synthesized derivatives of compound **27** based on the aminoisoquinoline pharmacophore (Supplementary Figure S8 and Supplementary Material). Among all the synthesized compounds (Compounds **837–841**), compounds **838** and **841** significantly increased EGFP intensity in IFN-γ dual fluorescence reporter (Figure 5A). Further, we confirmed that compounds **838** and **841** disrupted the RRM1/2-RNA interaction at concentrations of 12.28 μM and 1.52 μM, respectively (Figure 5B). In EMSA assay, compounds **838** and **841** disrupt RRM1/2/3 and RNA interaction (Figure 5C). Finally, compounds **838** and **841** was confirmed to decrease collagen I(α)1 and α-SMA expression in LX-2 cells (Figure 5D). According to the structure of compounds **27**, **838** and **841**, we speculated that 3-aminoisoquinoline pharmacophore is indispensable for compound disrupting activity. In addition, the amino group at position 7 in the isoquinoline was also important, as the deletion or substitution of amino groups caused reduced compound activity. While the halogen atom at position 1 in the isoquinoline had little effect on the activity of the compound compared between compounds **838** and **841**.

To confirm the selectivity of compounds **27**, **838**, **841** for CELF family, we performed an in-well protein-RNA binding assay, as showed schematically in Figure 6A. The platform showed a 5.3-fold signal-to-noise ratio, which indi-

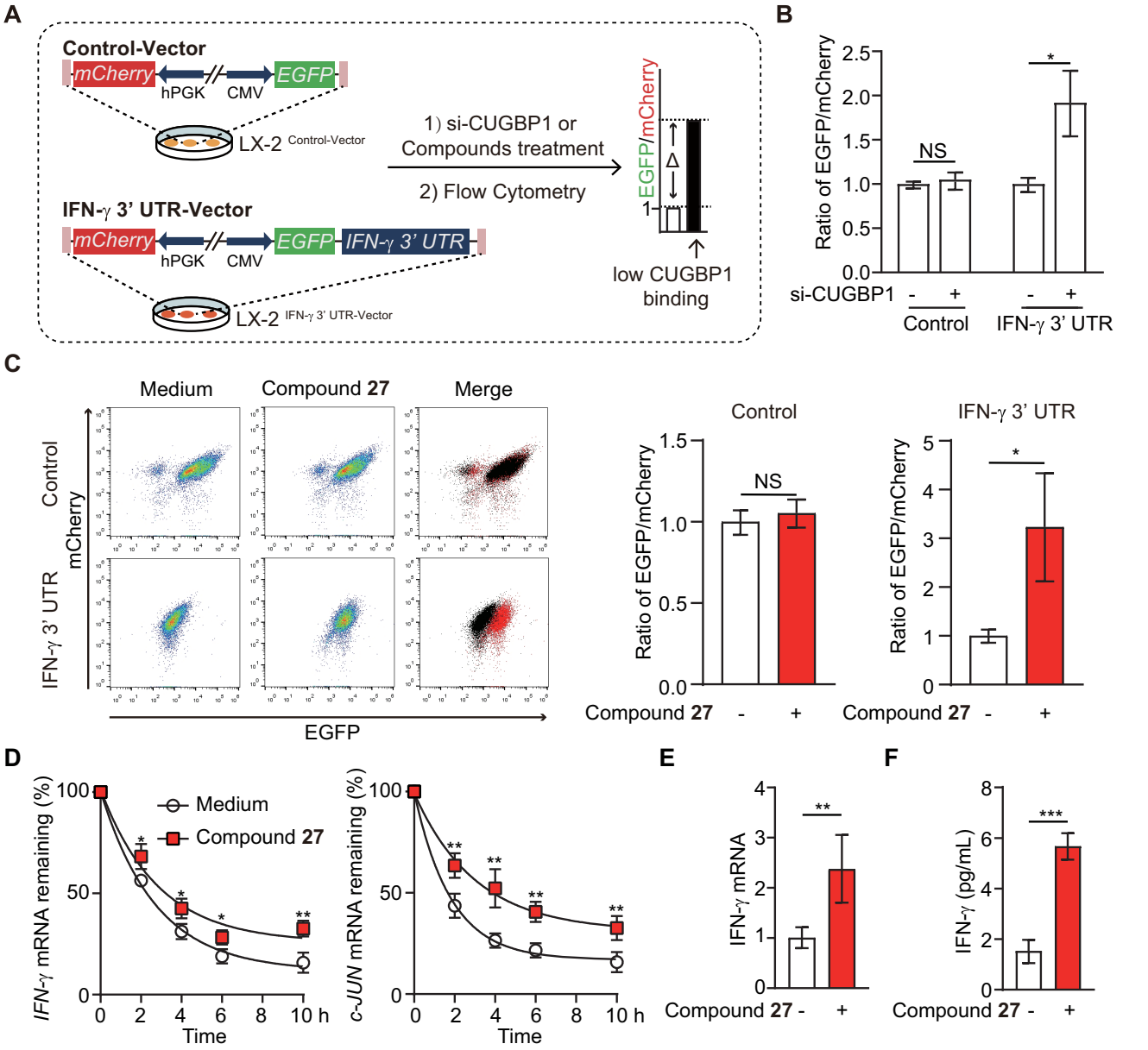

Figure 3. Compound 27 inhibits CELF1-mediated IFN-γ mRNA decay. (**A**) Plasmid construction of dual fluorescent reporter. Compared to the control vector, the IFN-γ mRNA 3′UTR was cloned downstream of EGFP in the IFN-γ 3′UTR reporter. (**B**) The ratio of EGFP/mCherry was tested in a dual fluorescent reporter treated with or without CELF1 small interfering RNA. (**C**) Flow cytometry analysis of compound **27** on a dual fluorescent reporter. (**D**) LX-2 cells were pre-treated with compound **27** for 6 hours and then co-treated with actinomycin D during the time course. Cells were collected for quantitative PCR analyses. (**E**) Quantitative PCR analyses of *IFN-γ* mRNA from LX-2 cells pre-treated with or without compound **27** and then co-treated with 5 ng/ml TGF-β1 for 12 h. (**F**) IFN-γ ELISA measurement of LX-2 supernatant treated with or without compound **27**. The data are representative of three independent experiments (mean ± SD). $^{*}P < 0.05$, $^{**}P < 0.01$, $^{***}P < 0.001$ by Student's *t*-test, NS, not significant.

cates that it is a good platform for further research (Figure 6B). Titration with increasing amounts of unlabeled GU RNA demonstrated the reversibility and specificity of the association (Figure 6C). Based on the in-well protein-RNA binding assay, we found that compound **27** induced a stronger inhibition of CELF1/2 than other CUG binding proteins (Figure 6D). Furthermore, we found that compound **841** is the most selective inhibitor of CELF1 (Figure 6D). In addition, compound **841** downregulated *COL1A1* and *ACTA2* mRNA expression and upregulated *IFN-γ* mRNA expression in a dose dependent manner (Figure 6E). Taken together, we identified compound **841** as a selective CELF1 inhibitor.

Next, we align the sequences of six CELF family proteins (CELF1-6) and found compound **27** binds S116, R148, E175 and C177 residues that were conserved in CELF1/2 but not in CELF3-6 (Supplementary Figure S9A), which explains the selectivity of compound **27**. In addition, compound **841** but not **27** is predicted to interact with I115 residue by docking (Supplementary Figure S9B–D), which may explain why compound 841 is more specific than compound 27 in targeting CELF1. In addition, a meta-analysis

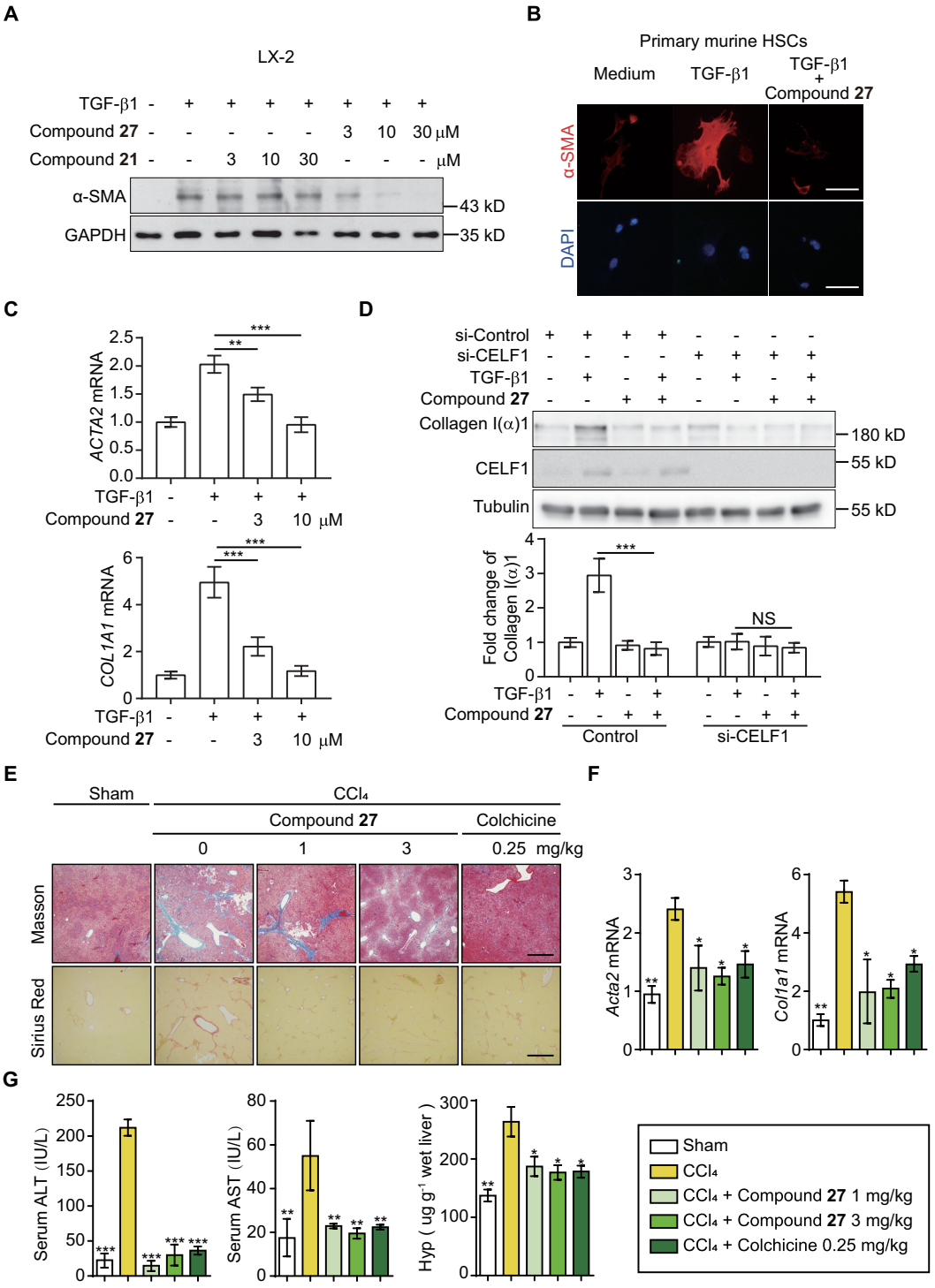

Figure 4. Compound 27 inhibits CELF1-mediated HSC activation and attenuates CCl_4-induced murine liver fibrosis. (**A**) Western blot analysis of α-SMA from LX-2 cells pre-treated with compound **21** or compound **27** for 6 h at the indicated concentration and then co-treated with 5 ng/ml TGF-β1 for 24 h. Compound **21** was used as a negative control. (**B**) Immunofluorescence analysis of α-SMA from primary mouse HSCs treated with or without 10 μM compound 27 and then treated with 5 ng/ml TGF-β1 for 24 h (Scale bars, 20 μm). (**C**) Quantitative PCR analyses of *ACTA2* and *COL1A1* from LX-2 cells pre-treated with or without compound **27** for 6 h and then co-treated with 5 ng/ml TGF-β1 for 12 h. (**D**) After transfection with si-CELF1 or control siRNA for 36 h, LX-2 cells were pre-treated with or without 10 μM compound **27** for 6 h and then co-treated with 5 ng/ml TGF-β1 for 24 h. Cell extracts were subjected to Western blot analysis. (E–G) A CCl_4-induced murine liver fibrosis model was generated in eight-week-old male ICR mice (eight to ten mice per group). Compound **27** was administered daily by intraperitoneal injection. Colchicine was administered daily by gavage. (**E**) Representative microphotograph of Masson-stained and Sirius Red-stained paraffin-embedded sections of liver tissues (Scale bars, 100 μm). (**F**) Quantitative PCR analysis of *Acta2* and *Col1a1* from mouse liver. (**G**) Expression levels of serum ALT, AST and liver Hyp. (F and G, mean ± SD; $n = 8$). $^*P < 0.05$, $^{**}P < 0.01$ and $^{***}P < 0.001$ versus the CCl_4 group by one-way analysis of variance followed by Dunnett's test. Data in **A, B, C, D** are representative of three independent experiments (mean ± SD); $^{**}P < 0.01$ and $^{***}P < 0.001$ by Student's *t*-test.

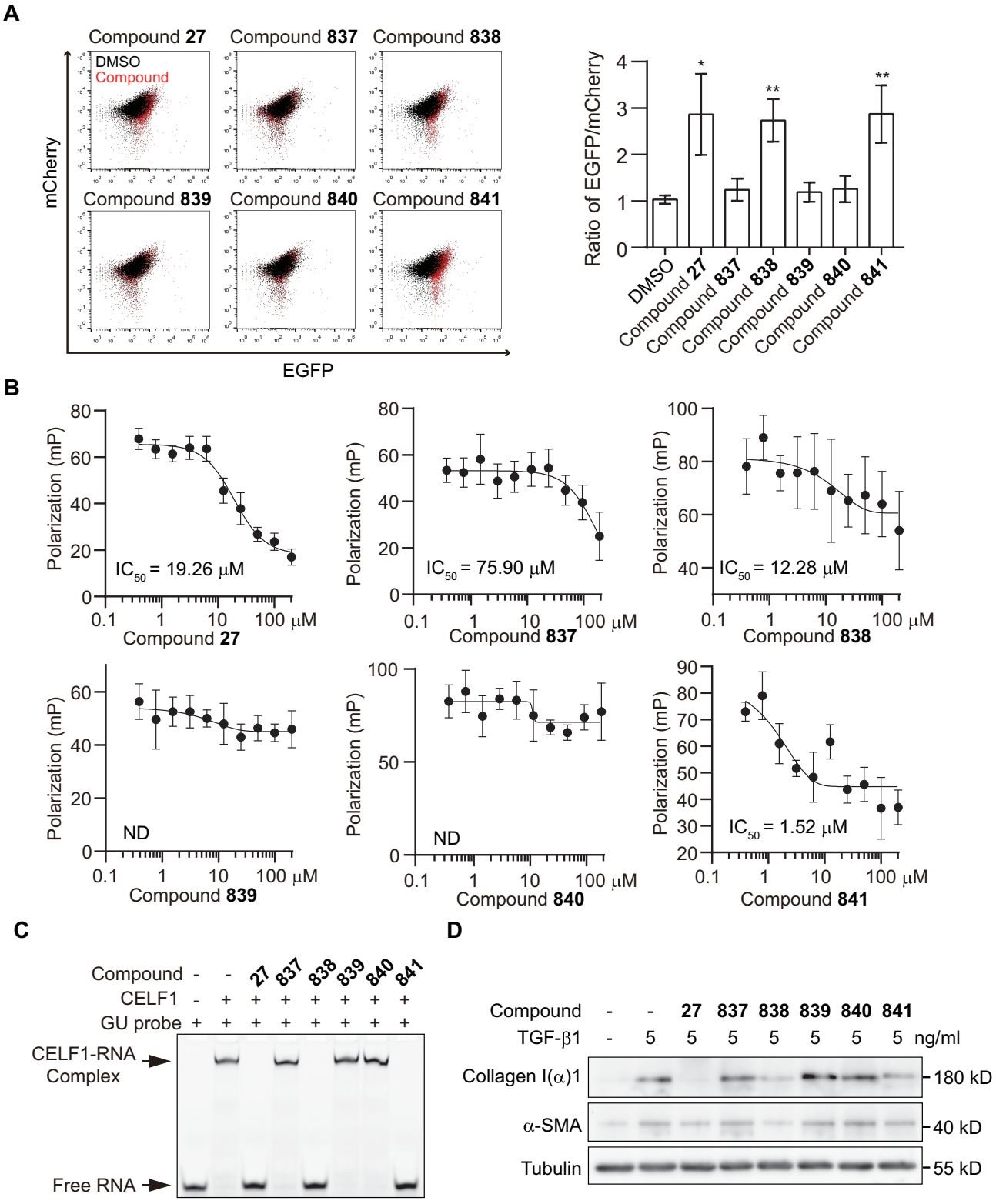

Figure 5. Structure-activity relationship of CELF1-RNA disruptors. (**A**) Flow cytometry analysis of compounds **27** and **837–841** on a dual fluorescent reporter. Quantitative analysis of the EGFP/mCherry ratio was show on right panel. (**B**) FP of compound **27** and **837–841** IC50 for RRM1/2-RNA binding inhibition. ND denotes the IC50 not determined. (**C**) EMSA assay analysis of compound **27** and **837**–**841** at 100 μM. (**D**) Western blot analysis of collagen I(α)1 and α-SMA from LX-2 cells pre-treated with compounds **27** and **837–841** for 6 h at 10 μM and then co-treated with 5 ng/ml TGF-β1 for 24 h. The data are representative of three independent experiments (mean ± SD). $^{**}P < 0.01$ by Student's *t*-test.

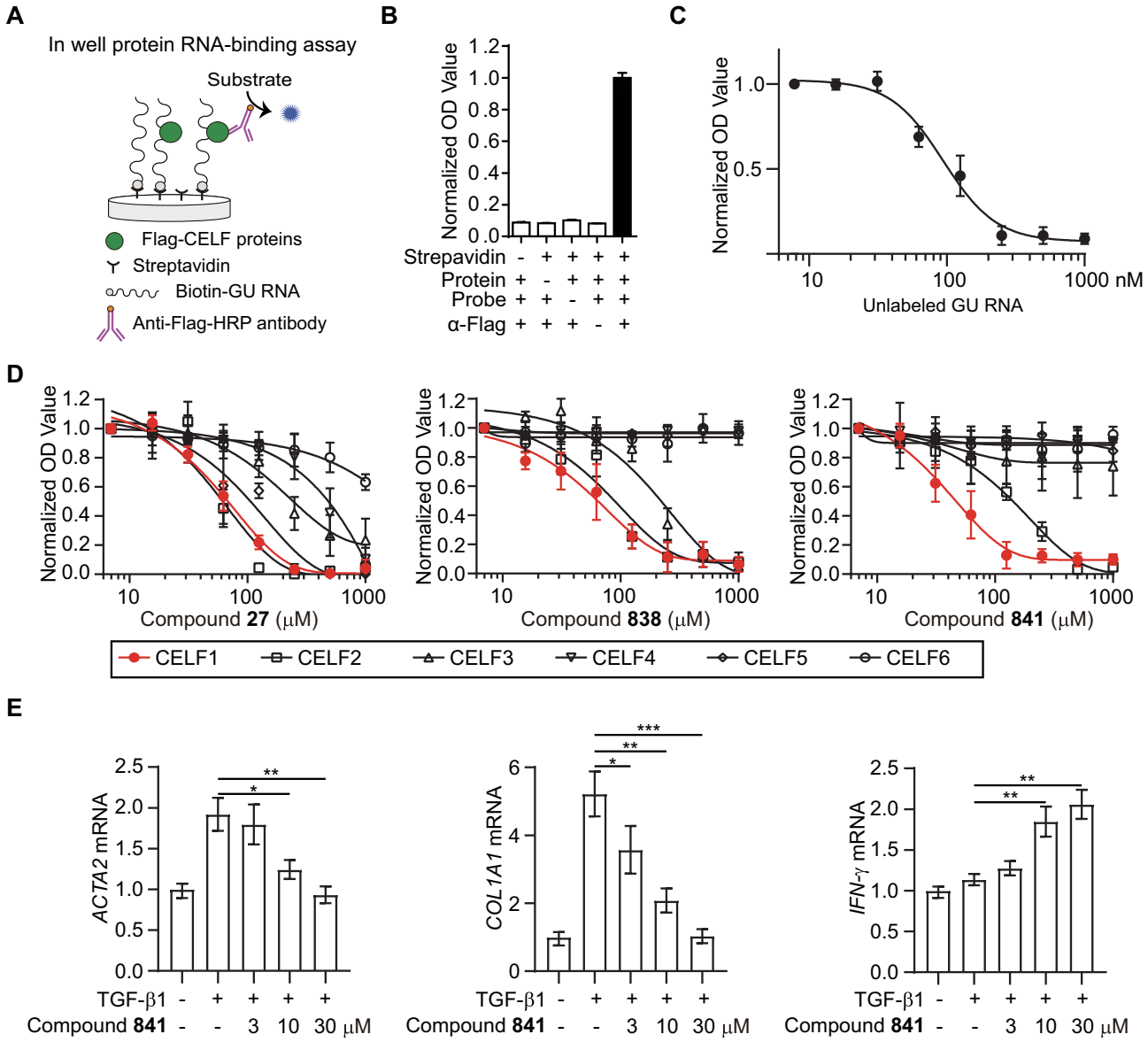

Figure 6. Identified compound 841 as a selective CELF1 inhibitor. (**A**) Schematic of in well protein RNA-binding assay. (**B**) The signal-to-noise ratio of the in well protein RNA-binding assay was confirmed by depleting strepavidin, probe, protein lysate and anti-Flag one by one. (**C**) Unlabelled GU RNA (Cold probe) efficiently displaced Biotin-GU probe in a dose-dependent manner. (**D**) The selectivity of compounds **27**, **838** and **841** was performed on in-well protein RNA-binding assay. (**E**) Quantitative PCR analyses of *COL1A1*, *ACTA2* and *IFN-γ* from LX-2 cells pre-treated with or without compound **841** for 6 h and then co-treated with 5 ng/ml TGF-β1 for 12 h. The data are representative of three independent experiments (mean ± SD). $^{*}P < 0.05$, $^{**}P < 0.01$, $^{***}P < 0.001$ by Student's *t*-test.

of all human RRM domains from RRM_1 (PF00076) family in Pfam database showed that the coincidence of I115 & C177 in CELF1 in RRM domain of CELF1 is rarely seen in other RRM domain-containing proteins (33) (Supplementary Figure S9E and Supplementary Table S2). These data suggest that compound **841** is a selective CELF1 inhibitor.

DISCUSSION

CELF1 is a key regulator of many diseases and is considered an attractive drug target. However, no small molecule inhibitors of CELF1 have been reported. Here, we screened and discovered that compound **27** was a disruptor of the CELF1-RNA interaction, with an IC_{50} value of 22.99 μM (Figure 1). Compound **27** showed unique pharmacological activity, restoring HSC homeostasis for the treatment of liver fibrosis via autocrine secretion of IFN-γ in activated HSCs. The pharmacological action of compound **27** proposed a novel therapeutic strategy for liver fibrosis.

CELF1 RRM2 contacts UGUU of the RNA segment via a network of direct and water-mediated hydrogen bonds and base-aromatic amino acid stacking interactions. The Watson–Crick and Hoogsteen edge of guanine are involved in two direct and one water-mediated hydrogen bonds. Experimental data showed that the substitution of guanines with either A, C or U in GU sequence (GUUGUUUUGUU) at position 4 and 10 caused undetectable binding to RRM1/2. This suggest the guanine is

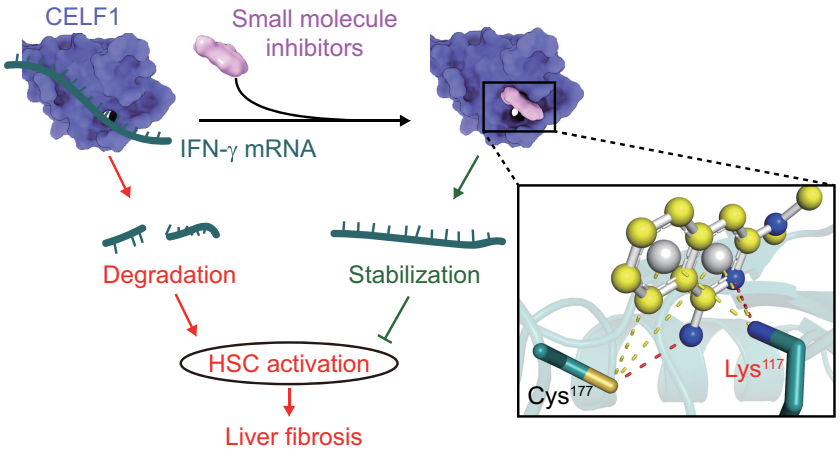

Figure 7. Disruption of CELF1-RNA binding by small molecule inhibitors for controlling HSC activation. CELF1 binds to IFN-γ mRNA 3′UTR and induces IFN-γ mRNA degradation. Loss of antifibrogenic IFN-γ further promotes HSC activation. Small molecule compound **27** directly binds to the RRM1/2 of CELF1 and disrupts the CELF1-RNA interaction, which blocks IFN-γ mRNA degradation. The upregulated antifibrogenic IFN-γ inhibits HSC activation and attenuates liver fibrosis.

important for GU RNA binding to RRM1/2 and this is why we performed *in silico* screening using the guanine binding site.

The discovery of CELF1 and CELF2 was based on their ability to bind $(CUG)_8$ oligonucleotides (34). CELF1 has the highest identity (> 90%) to CELF2 among CELF family members (35). Thus, it is challenging to inhibit CELF1 but not CELF2. Compound **27** showed the highest disrupting activity for targeting CELF1/2 compared with other CELF family members (Figure 6). Selectively targeting CELF1 RNA-binding activity may bring low side effects and be beneficial for further in vitro and *in vivo* tests. Understanding the structural basis of the CELF1–RNA binding interface is important for developing selective CELF1 inhibitors. The Lys117 residue of CELF1 was found to be important for the CELF1–RNA interaction by chemical shift perturbation analysis and crystal structure analysis (23,24,26). Consistently, we found that an arginine-to-alanine mutation at position 117 significantly reduced the binding of RRM2 to RNA by FP assay (Supplementary Figure S5). Furthermore, the Lys117 residue of CELF1 was also determined to be critical for the inhibition of CELF1-RNA binding by compound **27** (Figure 2E), which suggests that targeting CELF1 Lys117 is a potential solution for disrupting the CELF1-RNA interaction. Accordingly, derivatives of compound **27** that may target the Lys117 residue were further investigated. Compound **841**, a derivative of compound **27**, was identified as a selective CELF1 inhibitor (Figure 6D). We further found that the residue Ile115, which was predicted to be interacted with compound **841** but not **27** in our docked model, is specific to CELF1 compared with CELF2–6. These data suggest that targeting Ile115 in RRM2 maybe a strategy for developing specificity CELF1–RNA disruptor. In addition, we confirmed that the compound **27** has no interaction with RNA (Supplementary Figure S6). These data suggest compound **27** is a CELF1-specific inhibitor. While the possibility that compound **27** has an allosteric effect on CELF1 won't be rule out.

Inducing IFN-γ autocrine secretion in activated HSCs is a promising strategy for treating liver fibrosis. However, this strategy lacks appropriate pharmaceutical interventions. Subcutaneous injection of recombinant IFN-γ to treat liver fibrosis was investigated. However, it failed to reverse fibrosis in patients with advanced liver fibrosis or cirrhosis (36). There may be several reasons for the ineffectiveness of IFN-γ therapy. For example, recombinant IFN-γ is captured by IFN-γ receptors expressed in many non-HSCs. The short half-life of recombinant IFN-γ also limits its efficacy. Compared with recombinant IFN-γ, compound **27** has advantages. Compound **27** promotes IFN-γ expression in activated HSCs and controls HSC activation in an autocrine manner, which suggests that compound **27** could achieve high efficiency. Furthermore, knockdown of CELF1 is not able to induce IFN-γ expression in hepatocytes, liver sinusoidal endothelial cells, or Kupffer cells (4), which suggests that targeting CELF1 by compound **27** could selectively induce IFN-γ expression in activated HSCs. The cell selectivity of compound **27** presents good druggability profiles with fewer potential side effects. Thus, the discovery of compound **27** reveals a novel way to induce endogenous antifibrotic IFN-γ in activated HSCs for the treatment of liver fibrosis.

In conclusion, targeting CELF1 RNA-binding activity was achieved by small molecules, which promoted IFN-γ autocrine for controlling HSC activation (Figure 7). Targeting CELF1 RNA-binding activity may be a novel strategy for the treatment of liver fibrosis and other CELF1-related diseases.

DATA AVAILABILITY

Flow Cytometry experiments data (Figures 3C and 5A) have been deposited to the Flow Repository with the Repository ID: FR-FCM-Z4GS, FR-FCM-Z4GR and FR-FCM-Z4U6.

SUPPLEMENTARY DATA

Supplementary Data are available at NAR Online.

FUNDING

National Natural Science Foundation of China [81730100, 81874317, 82003783, 81722047, 21937005, 81670553]; National Key R&D Program of China [2017YFA0506000]; Fundamental Research Funds for the Central Universities [020814380161]; China Postdoctoral Science Foundation [2020M671445]. Funding for open access charge: National Natural Science Foundation of China.
Conflict of interest statement. None declared.

REFERENCES

1. Kuyumcu-Martinez,N.M., Wang,G.S. and Cooper,T.A. (2007) Increased steady-state levels of CUGBP1 in myotonic dystrophy 1 are due to PKC-mediated hyperphosphorylation. *Mol. Cell*, **28**, 68–78.
2. Chang,K.T., Cheng,C.F., King,P.C., Liu,S.Y. and Wang,G.S. (2017) CELF1 mediates connexin 43 mRNA degradation in dilated cardiomyopathy. *Circ. Res.*, **121**, 1140–1152.
3. Chaudhury,A., Cheema,S., Fachini,J.M., Kongchan,N., Lu,G., Simon,L.M., Wang,T., Mao,S., Rosen,D.G., Ittmann,M.M. *et al.* (2016) CELF1 is a central node in post-transcriptional regulatory programmes underlying EMT. *Nat. Commun.*, **7**, 13362.
4. Wu,X., Wu,X., Ma,Y., Shao,F., Tan,Y., Tan,T., Gu,L., Zhou,Y., Sun,B., Sun,Y. *et al.* (2016) CUG-binding protein 1 regulates HSC activation and liver fibrogenesis. *Nat. Commun.*, **7**, 13498.
5. Mulders,S.A.M., van den Broek,W.J.A.A., Wheeler,T.M., Croes,H.J.E., van Kuik-Romeijn,P., de Kimpe,S.J., Furling,D., Platenburg,G.J., Gourdon,G., Thornton,C.A. *et al.* (2009) Triplet-repeat oligonucleotide-mediated reversal of RNA toxicity in myotonic dystrophy. *Proc. Natl. Acad. Sci. U.S.A.*, **106**, 13915.
6. Lee,J.E. and Cooper,T.A. (2009) Pathogenic mechanisms of myotonic dystrophy. *Biochem. Soc. Trans.*, **37**, 1281–1286.
7. Goraczniak,R. and Gunderson,S.I. (2008) The regulatory element in the 3′-untranslated region of human papillomavirus 16 inhibits expression by binding CUG-binding protein 1. *J. Biol. Chem.*, **283**, 2286–2296.
8. Vlasova,I.A., Tahoe,N.M., Fan,D., Larsson,O., Rattenbacher,B., Sternjohn,J.R., Vasdewani,J., Karypis,G., Reilly,C.S., Bitterman,P.B. *et al.* (2008) Conserved GU-rich elements mediate mRNA decay by binding to CUG-binding protein 1. *Mol. Cell*, **29**, 263–270.
9. Siddam,A.D., Gautier-Courteille,C., Perez-Campos,L., Anand,D., Kakrana,A., Dang,C.A., Legagneux,V., Mereau,A., Viet,J., Gross,J.M. *et al.* (2018) The RNA-binding protein celf1 post-transcriptionally regulates p27Kip1 and dnase2b to control fiber cell nuclear degradation in lens development. *PLoS Genet.*, **14**, e1007278.
10. Katoh,T., Hojo,H. and Suzuki,T. (2015) Destabilization of microRNAs in human cells by 3′ deadenylation mediated by PARN and CUGBP1. *Nucleic Acids Res.*, **43**, 7521–7534.
11. Tsuda,K., Kuwasako,K., Takahashi,M., Someya,T., Inoue,M., Terada,T., Kobayashi,N., Shirouzu,M., Kigawa,T., Tanaka,A. *et al.* (2009) Structural basis for the sequence-specific RNA-recognition mechanism of human CUG-BP1 RRM3. *Nucleic Acids Res.*, **37**, 5151–5166.
12. Seki,E. and Schwabe,R.F. (2015) Hepatic inflammation and fibrosis: functional links and key pathways. *Hepatology*, **61**, 1066–1079.
13. Higashi,T., Friedman,S.L. and Hoshida,Y. (2017) Hepatic stellate cells as key target in liver fibrosis. *Adv. Drug Deliv. Rev.*, **121**, 27–42.
14. Bataller,R. and Brenner,D.A. (2005) Liver fibrosis. *J. Clin. Investig.*, **115**, 209–218.
15. Solano-Gonzalez,E., Coburn,K.M., Yu,W., Wilson,G.M., Nurmemmedov,E., Kesari,S., Chang,E.T., MacKerell,A.D., Weber,D.J. and Carrier,F. (2021) Small molecules inhibitors of the heterogeneous ribonuclear protein A18 (hnRNP A18): a regulator of protein translation and an immune checkpoint. *Nucleic Acids Res.*, **49**, 1235–1246.
16. Falese,J.P., Donlic,A. and Hargrove,A.E. (2021) Targeting RNA with small molecules: from fundamental principles towards the clinic. *Chem. Soc. Rev.*, **50**, 2224–2243.
17. Borgelt,L., Li,F., Hommen,P., Lampe,P., Hwang,J., Goebel,G.L., Sievers,S. and Wu,P. (2021) Trisubstituted pyrrolinones as small-molecule inhibitors disrupting the Protein–RNA interaction of LIN28 and Let-7. *ACS Med. Chem. Lett.*, **12**, 893–898
18. Wu,P. (2020) Inhibition of RNA-binding proteins with small molecules. *Nat. Rev. Chem.*, **4**, 441–458.
19. Baker,J.D., Uhrich,R.L., Strovas,T.J., Saxton,A.D. and Kraemer,B.C. (2020) Targeting pathological tau by small molecule inhibition of the poly(a):msut2 RNA-Protein interaction. *ACS Chem. Neurosci.*, **11**, 2277–2285.
20. Maji,B., Gangopadhyay,S.A., Lee,M., Shi,M., Wu,P., Heler,R., Mok,B., Lim,D., Siriwardena,S.U., Paul,B. *et al.* (2019) A high-throughput platform to identify small-molecule inhibitors of CRISPR-Cas9. *Cell*, **177**, 1067–1079.
21. Wang,L., Rowe,R.G., Jaimes,A., Yu,C., Nam,Y., Pearson,D.S., Zhang,J., Xie,X., Marion,W., Heffron,G.J. *et al.* (2018) Small-molecule inhibitors disrupt let-7 oligouridylation and release the selective blockade of let-7 processing by LIN28. *Cell Rep.*, **23**, 3091–3101.
22. Lightfoot,H.L., Miska,E.A. and Balasubramanian,S. (2016) Identification of small molecule inhibitors of the Lin28-mediated blockage of pre-let-7g processing. *Org. Biomol. Chem.*, **14**, 10208–10216.
23. Edwards,J.M., Long,J., de Moor,C.H., Emsley,J. and Searle,M.S. (2013) Structural insights into the targeting of mRNA GU-rich elements by the three RRMs of CELF1. *Nucleic Acids Res.*, **41**, 7153–7166.
24. Edwards,J., Malaurie,E., Kondrashov,A., Long,J., de Moor,C.H., Searle,M.S. and Emsley,J. (2011) Sequence determinants for the tandem recognition of UGU and CUG rich RNA elements by the two N–terminal RRMs of CELF1. *Nucleic Acids Res.*, **39**, 8638–8650.
25. Mori,D., Sasagawa,N., Kino,Y. and Ishiura,S. (2007) Quantitative analysis of CUG-BP1 binding to RNA repeats. *J. Biochem.*, **143**, 377–383.
26. Teplova,M., Song,J., Gaw,H.Y., Teplov,A. and Patel,D.J. (2010) Structural insights into RNA recognition by the alternate-splicing regulator CUG-binding protein 1. *Structure*, **18**, 1364–1377.
27. Ding,X., Zhao,Z., Wu,Y., Zhang,H., Chen,K., Luo,C., Luo,X. and Xu,H. (2021) Identification of novel anti-inflammatory nur77 modulators by virtual screening. *Bioorg. Chem.*, **112**, 104912.
28. David Rogers,M.H. (2010) Extended-Connectivity fingerprints. *J. Chem. Inf. Model.*, **50**, 742–754.
29. Siang,D.T.C., Lim,Y.C., Kyaw,A.M.M., Win,K.N., Chia,S.Y., Degirmenci,U., Hu,X., Tan,B.C., Walet,A.C.E., Sun,L. *et al.* (2020) The RNA-binding protein HuR is a negative regulator in adipogenesis. *Nat. Commun.*, **11**, 213.
30. Zhu,Y., Yang,L., Xu,J., Yang,X., Luan,P., Cui,Q., Zhang,P., Wang,F., Li,R., Ding,X. *et al.* (2020) Discovery of the anti-angiogenesis effect of eltrombopag in breast cancer through targeting of HuR protein. *Acta Pharm. Sin. B*, **10**, 1414–1425.
31. Jeong,W.-I., Park,O., Radaeva,S. and Gao,B. (2006) STAT1 inhibits liver fibrosis in mice by inhibiting stellate cell proliferation and stimulating NK cell cytotoxicity. *Hepatology*, **44**, 1441–1451.
32. Radaeva,S., Sun,R., Jaruga,B., Nguyen,V.T., Tian,Z. and Gao,B. (2006) Natural killer cells ameliorate liver fibrosis by killing activated stellate cells in NKG2D-dependent and tumor necrosis factor-related apoptosis-inducing ligand-dependent manners. *Gastroenterology*, **130**, 435–452.
33. Mistry,J., Chuguransky,S., Williams,L., Qureshi,M., Salazar,G.A., Sonnhammer,E.L.L., Tosatto,S.C.E., Paladin,L., Raj,S., Richardson,L.J. *et al.* (2021) Pfam: the protein families database in 2021. *Nucleic Acids Res.*, **49**, D412–D419.
34. Timchenko,L.T., Miller,J.W., Timchenko,N.A., DeVore,D.R., Datar,K.V., Lin,L., Roberts,R., Caskey,C.T. and Swanson,M.S. (1996) Identification of a (CUG)n triplet repeat RNA-binding protein and its expression in myotonic dystrophy. *Nucleic Acids Res.*, **24**, 4407–4414.
35. Vlasova-St Louis,I., Dickson,A.M., Bohjanen,P.R. and Wilusz,C.J. (2013) CELFish ways to modulate mRNA decay. *Biochim. Biophys. Acta*, **1829**, 695–707.
36. Pockros,P.J., Jeffers,L., Afdhal,N., Goodman,Z.D., Nelson,D., Gish,R.G., Reddy,K.R., Reindollar,R., Rodriguez-Torres,M., Sullivan,S. *et al.* (2007) Final results of a double-blind, placebo-controlled trial of the antifibrotic efficacy of interferon-gamma1b in chronic hepatitis C patients with advanced fibrosis or cirrhosis. *Hepatology*, **45**, 569–578.